



BNL-222935-2022-JAAM

Neural Lyapunov Control for Power System Transient Stability: A Deep Learning-Based Approach

Z. Tianqiao

To be published in "IEEE TRANSACTIONS ON POWER SYSTEMS"

April 2022

Interdisciplinary Science Department
Brookhaven National Laboratory

U.S. Department of Energy

USDOE Office of Electricity Delivery and Energy Reliability (OE), Power Systems Engineering
Research and Development (OE-10)

Notice: This manuscript has been authored by employees of Brookhaven Science Associates, LLC under Contract No. DE-SC0012704 with the U.S. Department of Energy. The publisher by accepting the manuscript for publication acknowledges that the United States Government retains a non-exclusive, paid-up, irrevocable, world-wide license to publish or reproduce the published form of this manuscript, or allow others to do so, for United States Government purposes.

DISCLAIMER

This report was prepared as an account of work sponsored by an agency of the United States Government. Neither the United States Government nor any agency thereof, nor any of their employees, nor any of their contractors, subcontractors, or their employees, makes any warranty, express or implied, or assumes any legal liability or responsibility for the accuracy, completeness, or any third party's use or the results of such use of any information, apparatus, product, or process disclosed, or represents that its use would not infringe privately owned rights. Reference herein to any specific commercial product, process, or service by trade name, trademark, manufacturer, or otherwise, does not necessarily constitute or imply its endorsement, recommendation, or favoring by the United States Government or any agency thereof or its contractors or subcontractors. The views and opinions of authors expressed herein do not necessarily state or reflect those of the United States Government or any agency thereof.

Neural Lyapunov Control for Power System Transient Stability: A Deep Learning-based Approach

Tianqiao Zhao, *Member, IEEE*, Jianhui Wang, *Fellow, IEEE*,
Xiaonan Lu, *Member, IEEE* Yuhua Du, *Member, IEEE*

Abstract—Power system control and transient stability analysis play essential roles in secure system operation. Control of power systems typically involves highly nonlinear and complex dynamics. Most of the existing works address such problems with additional assumptions in system dynamics, leading to a requirement for a complete and general solution. This paper, therefore, proposes a novel control framework for various power system control and stability problems leveraging a learning-based approach. The proposed framework includes a two-module structure that iteratively and jointly learns the candidate Lyapunov function and control law via deep neural networks in a learning module. Meanwhile, it guides the learning procedure towards valid results satisfying Lyapunov conditions in a falsification module. The introduced termination criteria ensure provable system stability. This control framework is verified through several studies handling different types of power system control problems. The results show that the proposed framework is generalizable and can simplify the control design for complex power systems with the stability guarantee and enlarged region of attraction.

Index Terms—Machine learning, power system stability, Lyapunov function, neural Lyapunov control

I. INTRODUCTION

STABILITY is the primary objective in the power system control and operation, concerning the capability to maintain the operating equilibrium after severe disturbances [1]. The increased penetration of renewable energy sources brings a variety of undesirable impacts and formidable challenges to power system control [2]. In this context, future power systems would be dominated by power electronic-interfaced small devices with different characteristics rather than some large synchronous generators (SGs) [3]. When a system is operated in such stressed conditions, different instability phenomena have emerged across the transient, frequency and voltage stability timescales [1]. This work aims to design a novel and general control approach to ensure stability in various power system applications.

The dynamics of power systems are usually highly complex and nonlinear. Numerous power system control methods have been reported in transient stability, frequency control and voltage control [4]–[9]. The transient stability is to maintain synchronism and usually assessed by conventional eigenvalue analysis and direct methods [1], or emerging passivity-based

methods [6]. However, these approaches require assumptions such that the power system is governed by large SGs, and needs to be dissipative. Frequency control ensures the power system frequency at its nominal value when the power balance fluctuates. It is generally implemented in a hierarchical architecture [10]. Various methods have been proposed to improve the frequency stability in the presence of load-side participation [9], uncertainties [5], and operational constraints [4]. Lastly, voltage control aims to prevent power system voltages from excessive fluctuations under either normal or disturbed conditions. It is typically analyzed by Lyapunov-based excitation control [8] or direct feedback linearization [11]. The effectiveness of these above methods is verified with additional assumptions on nonlinear and complex system dynamics for different forms of power system stability and control.

Furthermore, the concept of microgrids has been identified as a key element for future power systems. It brings both changes and challenges to traditional power systems since microgrids are usually dominated by inverter-based dynamics [12]. In current practice, droop methods have been widely adopted for microgrid stability analysis using different kinds of droop-based control [12]–[14]. In [12], a Lyapunov-based method is introduced to assess the droop-based microgrid stability. The performance of droop-based methods is further investigated and improved in [14]. The key element in droop-based control is the droop gain, where a higher gain leads to increased sensitivity to power injections but may induce system instability due to large frequency and voltage deviations from disturbances.

Overall, the control methodology and stability analysis need to be further developed for future power systems. However, these model-based approaches have additional requirements on the system, e.g., system positivity [6], lossless lines [7] and a special form of bus dynamics [12]. More importantly, their effectiveness highly relies on the system model to design an energy function that evaluates system stability. Therefore, any model inaccuracy would degrade system stability and control. The emerging learning-based approaches have recently gained attention in power system research, leveraging the advantage of the model-free feature and automatic knowledge extraction. The authors in [15] introduced an analysis tool for transient stability prediction based on deep learning. It solves a regression problem to predict the stability margin that evaluates system stability. The authors in [16] utilized deep reinforcement learning (DRL) to prevent a power system from ultra-low-frequency oscillations, which highly relies on

T. Zhao is with Brookhaven National Laboratory, Upton, NY 11973, USA (e-mail:tzhao1@bnl.gov).

J. Wang is with the Department of Electrical and Computer Engineering, Southern Methodist University, Dallas, TX 75275 USA (e-mail:jianhui@smu.edu)

X. Lu and Y. Du are with the College of Engineering, Temple University, Philadelphia, PA 19122 USA (e-mail: xiaonan.lu@temple.edu;tun22258@temple.edu).

a linearized system model. [17] embeds deep neural networks in a frequency-constrained scheduling problem in microgrid islanding events, admitting a mixed-integer formulation. However, the proposed framework is restricted to a specific problem with less adaptability. Although [18] and [19] address frequency and voltage control based on DRL respectively, their frameworks are sensitive to problem settings (e.g., control rewards).

Lyapunov function-based methods have been widely adopted for power systems for both stability analysis and control synthesis [6]–[8]. However, finding a valid Lyapunov function remains a challenge. Recently, learning-based methods show their effectiveness in handling nonlinear control problems in robotics [20] by learning a parametric control Lyapunov function through interacting with an unknown environment in an episodic learning framework. However, there still exist problems that impede their immediate use in power systems due to the numerical sensitivity, complex nonlinearity and extra operational requirements.

To summarize, existing literature faces emergent challenges when applied to future power systems. First, although a linearized small-signal model can guarantee asymptotic stability using a Lyapunov function, the design of these controllers based on the linearized model becomes unsuccessful when a large disturbance occurs. Furthermore, constructing a quadratic Lyapunov function is widely adopted to address transient stability problems. It could be conservative and restrict themselves to transmission networks ignoring the high R/X ratio in distribution networks, and meanwhile, they require specific system dynamics to achieve asymptotic stability. Lastly, most of the existing approaches focused on the transient stability of the system where the buses have the same dynamics. The authors in [21] developed stability conditions for power systems with heterogeneous bus dynamics. It still relies on the system passivity, and the stability condition requires the passivity index of each bus that is greater than a network index. Calculating this network index depends on the power flow and system operating conditions. It may provide conservative results and be sensitive to the modeling accuracy. Therefore, it is necessary further to develop approaches for power systems with heterogeneous bus dynamics.

This paper focuses on filling the existing gaps in designing feedback laws for various stability problems in power systems, capturing the core difficulty in power system transient stability and control. Inspired by [22], a deep learning-based control framework, Neural Power System Control, is developed for modern power systems. Our proposed approach utilizes neural networks to capture nonlinearity, which lifts dependence on linear or specific models. In addition, our approach directly handles various interface dynamics and rigorously satisfies the Lyapunov conditions by using neural networks. It is novel not in the use of machine learning but also in the combination of discovering Lyapunov functions and learning control laws simultaneously. It is more flexible to ensure the performance of control laws by adding simpler terms in the loss function to enlarge the region of attraction (ROA) on demand. The proposed framework consists of two modules: 1) Learning Module leveraging neural networks discovers parameters for

control and Lyapunov functions jointly; 2) Falsification Module utilizing a δ -complete-based algorithm [23] validates the candidate control law and Lyapunov function obtained from Learning Module and ensures the correctness of results. The main contributions are summarized as follows:

- A novel control framework is proposed by exploiting the advantage of neural networks and the completeness of satisfying nonlinear constraints to guarantee Lyapunov conditions fully. The model-free feature can deal with the stability problem in power systems with heterogeneous interface dynamics.
- The combination of the learning and falsification modules produces controllers with performance guarantees, i.e., the validated function holds the Lyapunov conditions in the verified state domain.
- Introducing regulator costs of a ROA to the learning process results in a significantly enlarged ROA for power system stability assessment.
- The feasibility and scalability of the proposed framework are demonstrated through several power control problems, i.e., transient stability and islanded microgrid control

II. PRELIMINARIES AND PROBLEM FORMULATION

This section introduces preliminaries and the problem formulation to facilitate the control design.

A. Lyapunov Function and Stability Conditions

Consider a controlled system governed by

$$\dot{x} = f(x, u), \quad (1)$$

where $f : \mathcal{X} \rightarrow \mathbb{R}^n$ is locally Lipschitz-continuous with \mathcal{X} being a path-connected state-space and $0 \in \mathcal{X}$. $x(t) \in \mathcal{X}$ is the state vector, and $\mathcal{K}(x) : \mathbb{R}^n \rightarrow \mathbb{R}^m$ is the feedback control law. Then the control synthesis problem is to design a feedback law $\mathcal{K}(x)$ so that all traces $x(\cdot)$ of the closed-loop system are asymptotically stable. To this end, we introduce the following definition.

Definition 1: For the system (1), a continuously differentiable function V is a Lyapunov function if the following condition holds for all $x \in \mathcal{X}$,

$$\begin{cases} V \text{ is positive definite and } V(0) = 0 \\ \min_{u \in \mathbb{R}} (\nabla_{f(x,u)} V) < 0 \end{cases} \quad (2)$$

where $\nabla_{f(x,u)} V$ is the Lie derivative of V over the vector field $f(x, u)$. If there exists a Lyapunov function V , it guarantees the existence of $\mathcal{K}(x)$ stabilizing the trajectories of a system to the equilibrium [24].

Definition 2: A controlled system (1) with equilibrium at the origin is asymptotically stabilizable, if there exists a continuously differentiable function V satisfying the conditions in (2).

B. Power System Model

1) *Bus Dynamic Model:* A network-reduced power system has n buses connected by transmission lines which is represented by the undirected graph $\mathcal{G} = (\mathcal{V}, \mathcal{E})$, where \mathcal{V} is the bus set and \mathcal{E} is the line set. Each bus includes a phasor voltage $V_i \angle \theta_i$ and a complex power injection $P_i + jQ_i$, where V_i and

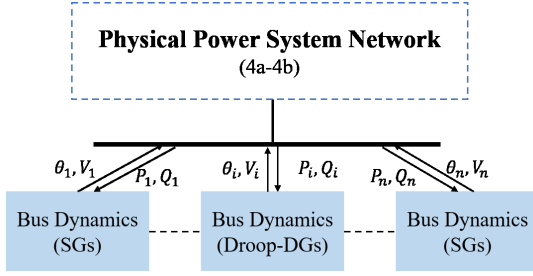


Fig. 1. The model of power system networks

θ_i are the voltage magnitude and angle of bus i , respectively; P_i and Q_i are active and reactive power injections of bus i , respectively. For a bus with a dynamic power resource, its dynamics can be described a dynamical relation which maps the complex power injection to the complex voltage [21]:

$$\begin{cases} \dot{x}_i = f(x_i, u_i) \\ y_i = C_i x_i \end{cases} \quad i \in \mathcal{V} \quad (3)$$

where $x_i = [\eta_i, \theta_i, V_i]$ and $y_i = C_i x_i = [\theta_i, V_i]$ with η_i being an auxiliary state indicating the corresponding dynamics of each device. The introduction of η_i facilitates modeling bus dynamics with heterogeneous devices. u_i is the control input to be designed later. Here, the load bus has no dynamics. However, the proposed solution can easily address the load-side frequency stability as in [25] following the control framework in Section III.

2) *Power Network Model*: The interconnection between each bus is represented by the admittance matrix. The power injections at bus i are denoted by

$$P_i^{\text{inj}} = G_{ii} V_i^2 + \sum_{j \in \mathcal{N}^j} V_i V_j (B_{ij} \sin(\theta_{ij}) + G_{ij} \cos(\theta_{ij})) \quad (4a)$$

$$Q_i^{\text{inj}} = -B_{ii} V_i^2 - \sum_{j \in \mathcal{N}^j} V_i V_j (B_{ij} \cos(\theta_{ij}) - G_{ij} \sin(\theta_{ij})), \quad (4b)$$

where \mathcal{N}^j is the set of adjacent buses to bus i ; G_{ij} and B_{ij} are the real and imaginary elements of the admittance matrix.

Combining (3) and (4), the power system is then modeled by a feedback loop between the network and dynamical behavior of each bus as in Fig. 1, which is written as the following compact form,

$$\begin{cases} \dot{x} = f(x, u) \\ y = Cx \\ u = \mathcal{K}(x) \end{cases} \quad (5)$$

where f is assumed to be a continuously differentiable function; $\mathcal{K}(x)$ is a control law which maps the states to system inputs. The aim is to design a control law, which stabilizes all state trajectories of a given power system.

Note that the definition of (5) covers various classes of bus dynamic models in power systems, such as classical synchronous generators [6], [9], inverter-interfaced power devices [3], and loads with frequency/voltage response [25]. Specific modelings and their effectiveness are demonstrated by several examples in Section IV. The following section will introduce a learning-based approach for power system transient stability.

III. LEARNING NEURAL POWER SYSTEM CONTROL

As outlined before, a Lyapunov function is needed in order to ensure the stability of (5) at hand. Discovering a Lyapunov function is generally computationally expensive subjecting to hard nonlinear constraints [20]. As shown in [26], [27], the nonlinearity and uncertainty can be handled by generic function approximators. This paper utilizes neural networks to embed the power system dynamics and provide a data-based solution to address the nonlinearity and uncertainty in solving power flow problems. To deal with this problem, this section presents a deep learning-based approach to search for a candidate Lyapunov function over a hypothesis space. Specifically, the Lyapunov function is parameterized by a parameter vector ϵ and defined by V_ϵ . For the sake of simplicity, we further denote Ψ for both the feedback law and the corresponding parameters which define the law.

Before presenting the main result, the following definitions are introduced.

Definition 3: (Compatible Sample) Given a training set $\mathcal{S} : \{x\}, x \in \mathcal{X}$, a set of compatible samples for an iteration is defined by

$$\mathcal{C} : \{(x, \Psi)\} \subset \mathcal{X} \times \mathcal{U}, \quad (6)$$

which includes both training and falsifier samples defined later.

Definition 4: (Falsifier Compatibility) A candidate V_ϵ is compatible with \mathcal{C} iff V_ϵ respects the conditions in Definition 1:

$$\exists x : x \neq 0 \wedge V_\epsilon(x) > 0 \wedge \nabla_{f(x, \Psi)} V < 0. \quad (7)$$

Note that the condition of $V(0) = 0$ is not included in Definition 4, and it will be guaranteed in advance using the ICNN feature in Learning Module. Given a power system governed by (5), the objective of neural power system control is to discover ϵ that ensures the existence of V_ϵ s.t. Definition 1, and synchronously returns a feedback control law stabilizing the system.

Fig. 2 outlines the developed architecture. It includes Learning Module and Falsification Module interacting in a training loop. Given a set of random samples $\mathcal{S} \subset \mathcal{X}$ at iteration k , Learning Module optimizes the weights ϵ of neural networks by back-propagating the Lyapunov risks (defined in Section III.A) and discovers a parametric V_ϵ to satisfy the conditions in Definition 1. The returned V_ϵ satisfies all the conditions, i.e., $V_\epsilon(0) = 0, V_\epsilon(s) > 0$, or $(\nabla_{f(s, u)} V(s)) < 0, \forall s \in \mathcal{S}$ but not necessarily over the entire region of \mathcal{X} . In sequence, Falsification Module reformulates the Lyapunov conditions following satisfiability modulo theories (SMT) and adopts an SMT solver (i.e., dReal [23]) to check whether the resulting V_ϵ violates the conditions over \mathcal{X} . If any violation exists, the SMT solver in Falsification Module generates the counterexamples x_{violated} that violate either $V_\epsilon(x_{\text{violated}}) > 0, (\nabla_{f(x_{\text{violated}}, u)} V(x_{\text{violated}})) < 0$. These samples are added to the sample set \mathcal{S} for the next learning iteration $k+1$. With the updated sample set, Learning Module is enforced to discover a new candidate. The new V_ϵ is fed to Falsification Module again, forming a training loop. The loop repeats until Falsification Module certifies that no violated samples exist, which proves the correctness of V_ϵ .

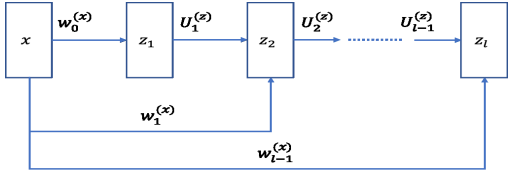


Fig. 3. Input convex neural networks [28]

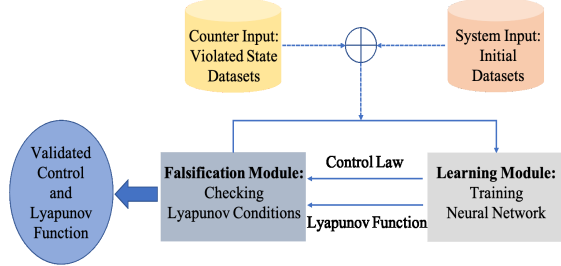


Fig. 2. The control diagram

A. Learning Module

With a training set \mathcal{S} , the objective is to construct a candidate Lyapunov function V_ϵ satisfying the conditions in Definition 1. Here, we will present a technique to discover both control and Lyapunov functions at the same time, by which the system stability can be ensured rigorously by the Lyapunov conditions.

The Lyapunov conditions can be described by:

- 1) $V_\epsilon(0) = 0$
- 2) $V_\epsilon > 0$
- 3) $\nabla_{f(x,\Psi)} V_\epsilon(x) < 0$.

In addition, the property of a Lyapunov function requires only the local optima at 0. To enforce this constraint, we represent $V_\epsilon(x)$ by utilizing an input convex neural network (ICNN) function g [28] in Learning Module, and the structure of ICNN is given in Fig.3. It updates the parameters for ϵ and Ψ simultaneously to improve the likelihood of non-violations, such as

$$\begin{aligned} z_1 &= \varrho_0(w_0x + b_0), \\ z_{i+1} &= \varrho_i(U_i z_i + w_i x + b_i), \quad i = 1, \dots, l-1, \\ g(x) &= z_l, \end{aligned} \quad (8)$$

where w_i and U_i are the real-valued and positive-valued weights respectively, and b_i is a real-valued bias. ϱ_i is a convex, monotonically non-decreasing non-linear activation function. Note that the non-smooth ReLu cannot be used in this network because the Lyapunov conditions have to be determined through their Lie derivatives such as

$$\Delta V_\epsilon = \frac{\partial V}{\partial x} = \prod_{k=1}^{i-1} \frac{\partial z_i}{\partial z_{k-1}}. \quad (9)$$

To address this issue, we adopt a smoothed ReLU as used in [29] to make the Lyapunov function continuously differentiable. Since g is convex in x [28], a single optimum of V_ϵ is guaranteed, and V_ϵ is defined by

$$V_\epsilon = \varrho_{i+1}(g(x) - g(0)) \quad (10)$$

where we shift V_ϵ to ensure (1) $V_\epsilon(0) = 0$. The learned Lyapunov function needs to satisfy all conditions in (2).

Learning Module will update both ϵ and Ψ to improve the likelihood of constraint satisfaction. The design problem can be written as the minimization of the following min-max cost,

$$\inf_{\epsilon, \Psi} \sup_{x \in \mathcal{X}} \left(\alpha \max(0, -V_\epsilon(x)) + \beta \max(0, \nabla_{f(x,\Psi)} V_\epsilon(x)) \right). \quad (11)$$

where α and β are the tunable parameters. (11) is the cost conceptually indicating any violation of Lyapunov conditions over the state space. The first term on RHS of (11) is the penalty of the violation of the second condition in Lyapunov conditions (i.e., $V_\epsilon > 0$), and the second term is to penalize the violation of the third condition (i.e., $\nabla_{f(x,\Psi)} V_\epsilon(x) < 0$). The minimal zero-loss of (11) indicates that the learned function satisfies all the Lyapunov conditions with a valid controller.

Note that the difficulty in calculating (11) is to estimate the violation of the Lyapunov conditions and meanwhile, to ensure the estimation over the entire state space. Discovering all the estimations may be computationally intractable for a large-dimensional space or deep networks during the learning process. Therefore, inspired by [22], we propose the Lyapunov-like cost that defines the expected cost with the learned Lyapunov function and control law, evaluated by the sampled state over the state space at each learning step.

Definition 5: (Lyapunov-like Cost) For a candidate V_ϵ , the Lyapunov-like cost is a defined by

$$L(\epsilon, \Psi)_\rho = \mathbb{E}_{x \sim \rho(\mathcal{X})} \left(\alpha \max(0, -V_\epsilon(x)) + \beta \max(0, \nabla_{f(x,\Psi)} V_\epsilon(x)) \right), \quad (12)$$

where x is sampled over \mathcal{X} with a distribution ρ . (12) can be estimated through Monte Carlo simulation, i.e.,

$$L(\epsilon, \Psi)_{N,\rho} = \frac{1}{N} \sum_{k=1}^N \left(\alpha \max(0, -V_\epsilon(x_k)) + \beta \max(0, \nabla_{f(x_k,\Psi)} V_\epsilon(x_k)) \right), \quad (13)$$

where $x_k, k = 1, \dots, N$, are the samples of \mathcal{X} over ρ .

One important metric for controller performance is its ROA. The ROA is a forward invariant set containing the origin, in which all possible system trajectories will never leave. When a disturbance occurs, the ROA for a power system is a region in which the operational status (e.g., rotor angles and frequencies) can converge to the stable equilibrium [30]. Therefore, one can enhance the power system robustness to a disturbance through maximizing the ROA of a power system. Similar to [22], two loss items are added to the Lyapunov-like cost. The loss items measure the increasing rate of the Lyapunov function subject to the radius of the level sets. The ROA-Lyapunov-like cost is given by

$$L(\epsilon, \Psi)_{N,\rho} + \frac{1}{N} \sum_{k=1}^N \|x_k\|^2 - cV_\epsilon(x_k), \quad (14)$$

where c is a positive parameter. Learning Module learns a pair of Ψ and V_ϵ . However, the learned V_ϵ needs not necessarily be a Lyapunov function since the limited samples do not cover all states in \mathcal{X} . To overcome this problem, the following falsification module is introduced.

B. Falsification Module

With the pair (V_ϵ, Ψ) obtained in Learning Module, this module implements a falsification process. It includes three steps:

- i) Check the Lyapunov conditions in (2)
- ii) Seek any violated states
- iii) Generate an updated training set \mathcal{S}_k and store Compatible Sample as in Definition 3.

An SMT problem is formulated over real numbers for formal verification. In particular, V_ϵ is a Lyapunov function if the following first-order logic formula is satisfied,

$$V_\epsilon(x) > 0 \wedge \nabla_{f(x, \Psi)} V_\epsilon(x) < 0, \quad x \in \mathcal{X} \setminus 0,$$

However, solving large and quantified formulas can be time-consuming generally. To this end, we rewrite this formula to smaller satisfiability queries that can be solved efficiently by an SMT solver in practice. Specifically, we consider the dual falsification problem as

$$\underbrace{(V_\epsilon(x) \leq 0, \quad x \in \mathcal{X} \setminus 0)}_{\varphi_1} \vee \underbrace{(\nabla_{f(x, \Psi)} V_\epsilon(x) \geq 0, \quad x \in \mathcal{X} \setminus 0)}_{\varphi_2}, \quad (15)$$

which is a nonlinear constraint satisfaction problem to determine the existence of counterexamples. Therefore, we only need to verify two independent satisfiability queries, i.e., if either φ_1 or φ_2 is true. If any of them is true, an SMT solver returns the violated samples for either of them, and the results of each of the two formulas constitute the violated sample set, i.e., $\mathcal{S}_k := \mathcal{S}_{k-1} \cup \{(x_{a,k})\}$, where $(x_{a,k})$ is the violated sample at iteration k . On the other hand, if both of them have unsatisfied results, no samples will be returned, and the corresponding Lyapunov function is validated $\forall x \in \mathcal{X}$. With the repression of the original formula, we can speed up the verification process.

Note that solving an SMT formula with nonlinear constraints is NP-hard and computationally expensive. The recently developed SMT solver over reals, dReal [31], is adopted in this work to handle this problem. The correctness and completeness of violation reporting are guaranteed by the "δ-complete" defined in [23]. A δ-complete algorithm returns a δ-weakening answer such as 1) (15) has no solution; 2) a solution satisfies (15). Note that δ-weakening is a syntactic relaxation of the original problem where if the original problem is satisfied, the δ-weakening is always satisfied [23]. The detailed effects of the δ selection on the algorithm can be found in [31].

C. Termination

Recall that in the proposed framework, Learning Module provides a learned Lyapunov function, and Falsification Module refutes this function by reporting any violated states and appends them into the training set. For a given Compatible set \mathcal{C} , the learning process is terminated when the dReal solver computes $\varphi(x)$ that is unsatisfying δ-complete in Falsification Module. A successful learning process returns a valid Lyapunov function which satisfies (2) and stabilizes (5). In other words, the learning algorithm succeeds if Falsification Module can not return any counterexample that violates Falsifier

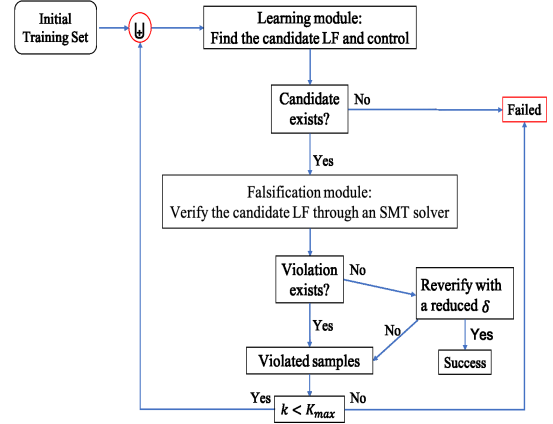


Fig. 4. The control flowchart

Compatibility. Thus, Theorem 3.1 concludes that the candidate function is a valid Lyapunov function.

Theorem 3.1: Considering the system (5) with a control policy u with f being continuously differentiable, and the initial states $x_0 \subset \mathcal{X}$, $V_\epsilon(x)$ is a Lyapunov function, and then Ψ is the corresponding control policy iff Falsification Module returns an empty set.

Proof: See Appendix.A ■

Note that when the learning process is terminated, the returned solution will be rechecked by a much smaller δ to verify its correctness and robustness further. If there is a violation using this smaller δ , these counterexamples will be added to the training set, and the learning process is restarted until meeting the termination condition.

Remark 3.1: The proposed solution deploys neural networks in Learning Module to equip our solution with the model-free feature. In sequence, Falsification Module ensures the correctness of the learned results building on the δ-completeness of an SMT solver [31]. Combining the above two modules equips our solution with the robustness to model uncertainties. Note that the uncertainty would not only from the model development, but also from external disturbances. The influence of external disturbances will be investigated in our future work.

Remark 3.2: The time-delay effect on the system stability has been investigated in [32]. The influence of time-delay on system stability could be potentially integrated in our framework by 1) changing the Lyapunov-like cost representing Lyapunov conditions for a system with no delay to a cost representing Lyapunov conditions for a time-delayed system and 2) generating sample data from the time-delayed system.

D. Solution Implementation

The flowchart of the proposed framework is shown in Fig. 4. The learning process works until not satisfying the δ-complete or exceeding the maximum learning iteration K_{\max} . At iteration k , Learning Module contains a training set

$$\mathcal{S}_k := \{x_1, \dots, x_k\} \subset \mathcal{X}. \quad (16)$$

Accordingly, ϵ_k defines the set of candidate parameters for $V_{\epsilon_k}(x)$ similar to Ψ_k . The aim is to learn a set of parameters

respecting Falsifier Compatibility, i.e.,

$$\epsilon_k : \left\{ \epsilon \mid \bigwedge_{(x_k, \Psi_k) \in \mathcal{C}_k} V_\epsilon(x_k) > 0 \wedge \nabla f_{(x_k, \Psi_k)} V_\epsilon(x_k) < 0 \right\}. \quad (17)$$

Starting from an initialized sample set $\mathcal{S}_0 \neq \emptyset$ and ϵ_0 , the learning procedure includes the following steps.

1. Find the candidate Lyapunov function and control law: given a learning period T_l and \mathcal{S}_k , Learning Module computes the candidate $V_{\epsilon_{T_l}}(x)$ and Ψ_k , i.e., for $j = [1, \dots, T_l]$,

$$\begin{aligned} V_{\epsilon_j}(x), \Psi_j(x) &\leftarrow \text{Neural networks}(x), \forall x \in \mathcal{S}_k \\ \epsilon_j, \Psi_j &\leftarrow \text{Lyapunov-like cost minimization} \end{aligned} \quad (18)$$

2. Verify the candidate: Falsification Module tests whether $V_{\epsilon_{T_l}}(x)$ is a validated Lyapunov function over \mathcal{C}_k , i.e.,
 - a. Reformulate the condition (15) in the dReal format and utilize the SMT solver to check condition violation
 - b. Return the satisfiability, results and all violated samples if they exist.
3. Check the termination condition:
 - a. If true, it terminates the learning process and return $V_{\epsilon_{T_l}}(x)$ and Ψ_k .
 - b. Otherwise, it reports all violated samples $\{x_{\text{violated}}\}$ to Learning Module.
4. Update the training set: all violated samples are added to the training set to produce the next learning iteration:

$$\mathcal{S}_{k+1} : \mathcal{S}_k \cup \{x_{\text{violated}}\}. \quad (19)$$

The δ - complete guarantees the obtained $V_{\epsilon_{T_l}}(x)$ is a Lyapunov function and holds for all states in the state space \mathcal{X} , along with a stabilizer Ψ_{T_l} .

Note that the interaction frequency between Learning Module and Falsification Module is one of the essentials that affects the convergence speed. Adding violated samples too frequently might result in overfitting learning results since these samples resemble each other. To overcome this issue, additional random samples from a neighborhood of x_{violated} are appended to \mathcal{S}_{k+1} as well. These samples do not need to be the solution of (15). The introduced expedient does not hinder the overall soundness of the solution but further enhances its performance and generalization.

Remark 3.3: It should be noted that our framework could potentially facilitate the assessment of small-signal stability. In particular, we consider linearized power system dynamics that are widely adopted in analyzing small-signal stability [3], [7], and our framework can discover a corresponding Lyapunov function. With the learned Lyapunov function, we can estimate the security region to certify system small-signal stability following [7].

IV. CASE STUDIES

In this section, we demonstrate the proposed solution that can be potentially adapted to various power system control objectives. In particular, we illustrate two widely adopted

TABLE I
HYPERPARAMETERS

	Application I	Application II	Application III
α	0.25	0.25	0.25
β	0.42	0.36	0.53
c	0.01	0.01	0.02
Learning rate	0.01	0.01	0.01
K_{learning}	100	100	100
K_{max}	5000	8000	8000
δ (training)	0.05	0.05	0.05
δ (testing)	0.01	0.01	0.01
Initial sample size	300	1000	2000
Solver	Adam		

examples in power system control and stability: i) power system transient stability; ii) islanded microgrid control.

The hyperparameters used in each case are listed in Table I. The performance of our solution is mainly decided by the parameters of α and β . We provide an empirical procedure to tune these parameters. Given an initial guess of α and β , let V_ϵ be the candidate function at iteration k . We can visualize the results of V_ϵ and its derivative numerically, by which we may determine the direction to tune some of the parameters based on the violation(s) of Lyapunov conditions. Specifically, after the k iterations, we visualize the learned ϵ_k and its derivative respecting \mathcal{X} . Then, we can tune the parameters based on the visualization. For example, suppose the visualization of ϵ_k returns a positive V_ϵ , but the derivative of V_ϵ is non-negative, we will fix the other parameters and increase β to recheck their selections.

In the first two cases, the neural networks have 5 layers, and the number of nodes in layers is set as $x_n - 4x_n - 4x_n - 4x_n - 1$, where x_n is the dimension of states. In the last case, it has 6 layers, and the number of nodes in layers is set as $x_n - 6x_n - 6x_n - 6x_n - 6x_n - 1$. The input features are system states, and the output feature is V_ϵ . The parametric variables of neural networks are trained using subgradient-based methods. We introduce auxiliary control variables in system dynamics to fulfill the control objective. For instance, an auxiliary control variable is introduced to stabilize the system following [33] in Application I. In Application II, we introduce two control variables in the droop-based dynamics to regulate microgrid frequency and voltage following [13]. To generate the initial data set in Fig. 2, we sample a set of initial points from \mathcal{X} , e.g., \mathcal{S}_t , and feed them to the system dynamics to obtain the evaluation of states for only one step, e.g., \mathcal{S}_{t+1} . All numerical studies are learned and performed in Python on a personal laptop.

A. Application I: Power system transient stability

In this application, the proposed solution is applied to design the Lyapunov function and corresponding control law to ensure power system transient stability. Following [7], we assume that the interface voltage is constant in the transient period due to its much slower dynamical behaviors. The dynamics of a

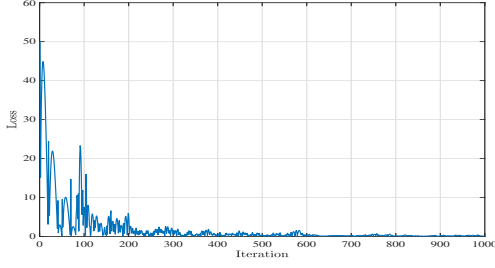


Fig. 5. Training loss

power system are governed by the following swing equation [7], i.e.,

$$m_i \ddot{\theta}_i + d_i \dot{\theta}_i + \sum_{j \in \mathcal{N}^j} B_{ij} V_i V_j \sin(\theta_i - \theta_j) - p_i = 0, \quad (20)$$

where θ_i is the angle of the generator at bus i ; m_i and d_i are inertia and damping coefficients of a generator, respectively; p_i is the mechanical power. For a load bus, we let $m_i = d_i = 0$. Here, we transfer the states to steady states to obtain a perturbed model,

$$m_i \ddot{\tilde{\theta}}_i + d_i \dot{\tilde{\theta}}_i - u_i + \sum_{j \in \mathcal{N}^j} B_{ij} V_i^* V_j^* [\sin(\theta_{ij}^*) - \sin(\theta_{ij}^* - \tilde{\theta}_{ij})] = 0, \quad (21)$$

where we denote $\tilde{\theta}_i = \theta_i - \theta_i^*$, $\tilde{\theta}_{ij} = \tilde{\theta}_i - \tilde{\theta}_j$, and $\theta_{ij}^* = \theta_i^* - \theta_j^*$ with \square^* being the steady-state value. In the steady state, $p_i = \sum_{j \in \mathcal{N}^j} B_{ij} V_i^* V_j^* \sin(\theta_{ij}^*)$. The feedback control law u_i is added that stabilizes the system at the origin.

Remark 4.1: This case study adopts the classical swing equation which is widely utilized to capture the power system dynamics sufficiently well [34]. Note that following [35], [36] the augmented damping term can represent the effects of generator excitation control. Besides, following a similar line in Application I, the proposed solution is applicable to other types of SG models as long as the basic knowledge of the system order and the sampled data of system states are available.

The proposed solution is tested on the IEEE 39-bus system with 10 machines, and the system parameters are taken from [37], where we decrease the inertia of SGs to model the unstable feature. Assuming Bus 31 is the swing bus, the proposed solution controls the dynamics of the other 9 machines. The objective of the transient stability is to learn a control law u_i that can ensure system stability while maximizing its ROA. The training loss is given in Fig. 5. In Fig. 6, it includes the evaluation of all system states. The two figures at the top are the original system trajectories without control, and the other two figures at the bottom are the system trajectories after applying the proposed solution. It should be noted that some of the original trajectories are unstable, and with the proposed solution, these trajectories are stabilized and converging to the equilibrium.

Figs. 7(a)-7(b) visualize the validated Lyapunov function of SG 1, which verify the proposed solution can ensure the existence of a Lyapunov function satisfying the conditions in (2) in an operation region. We show the resulting trajectories

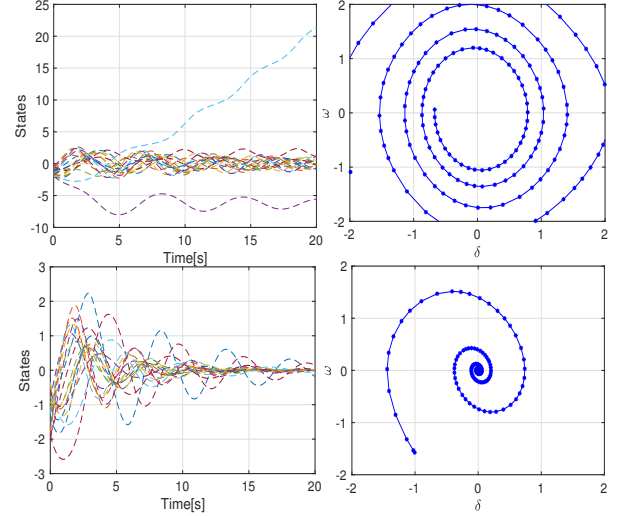
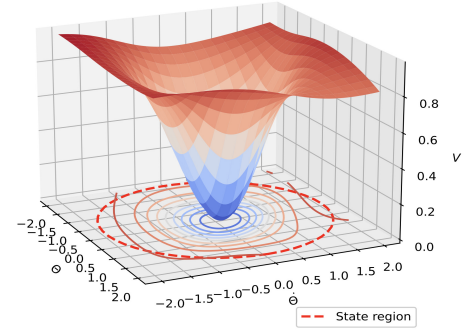
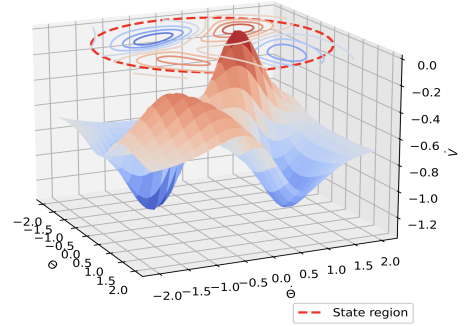


Fig. 6. System trajectories of IEEE 39-bus system in Application I



(a) Learned Lyapunov function



(b) The derivative of the learned Lyapunov function

Fig. 7. The results of SG 1 in Application I: $V_\epsilon > 0$ in the upper figure and $\nabla_{f(x,\Psi)} V_\epsilon < 0$ in the lower figure

of two example SGs (i.e., SG 1 and SG 5) that have the typical system trajectories, where SG 1 is unstable at the origin and SG 5 has a different attractor from the origin (see Figs.8(a)-8(b)). After applying the learned control law, the resultant trajectories of SG 1 and SG 5 are given in Fig. 9(a) and Fig. 9(b), respectively. As in Figs. 9(a)-9(b), the trajectories of both SGs converge to the origin, and in other words, they are stabilized by our solution (see Fig.6).

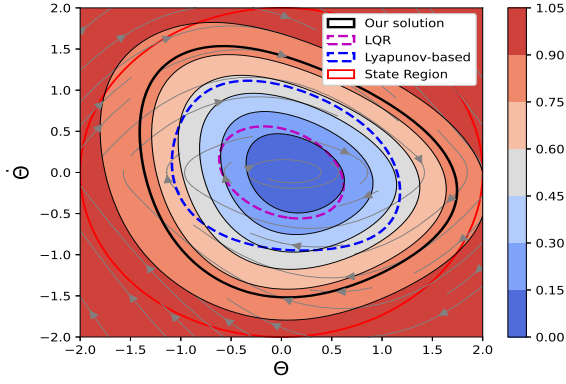


Fig. 10. The estimated ROA for SG 1 in Application I

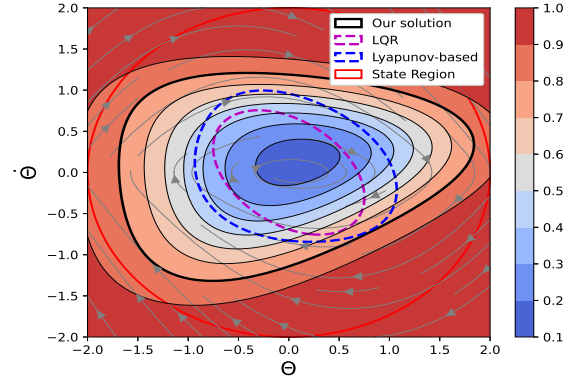


Fig. 11. The estimated ROA for SG 5 in Application I

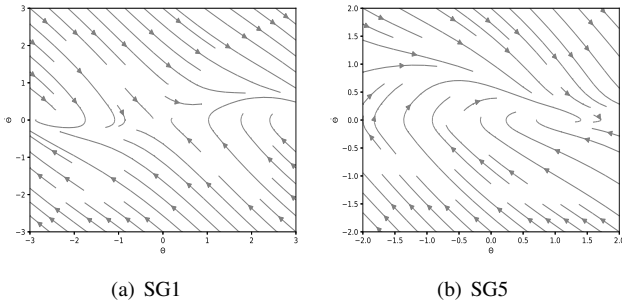


Fig. 8. The original vector fields of two example SGs in Application I

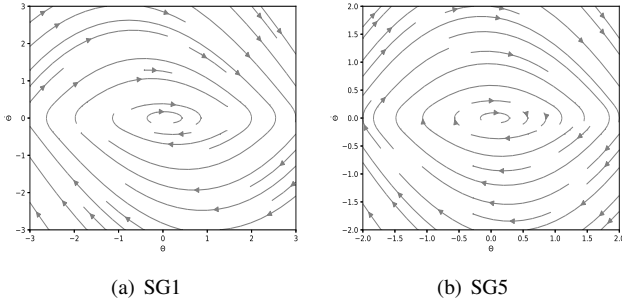


Fig. 9. The regulated vector fields of two example SGs in Application I

Furthermore, we compare our solution with an LQR-based approach [38] and a recent Lyapunov-based approach [30] to demonstrate the ability to learn a larger ROA. The ROA for power systems provides a valuable analysis tool of the stability level, referring to a subspace of states that can converge to an equilibrium. The results in Figs. 10 - 11 illustrate the estimated ROA, verifying the proposed solution enlarges the estimated ROA significantly.

B. Application II: Islanded microgrid control

In this case, we consider the bus dynamics that are governed by inverter-interfaced DGs in an islanded microgrid. Suppose a DG is controlled by $P - \omega$ and $Q - V$ droop controllers following [13],

$$\dot{\theta}_i = \omega_i \quad (22a)$$

$$\tau_\omega \dot{\omega}_i + (\omega_i - \omega_{\text{ref}}) = -\sigma_\omega P_i + u_{p,i} \quad (22b)$$

$$\tau_v \dot{V}_i + (V_i - V_{\text{ref}}) = -\sigma_v Q_i + u_{q,i} \quad (22c)$$

where τ_ω and τ_v are the time constants, and σ_ω and σ_v are the $P - \omega$ and $Q - V$ control gains, respectively. As the droop-based control is a basic proportional controller, two feedback laws $u_{p,i}$ and $u_{q,i}$ are added to be learned. They play the role of secondary controllers following [39]. The objective of (22) for a DG is to achieve its frequency and voltage regulation such as $\omega_i \rightarrow \omega_{\text{ref}}$ and $V_i \rightarrow V_{\text{ref}}$, where ω_{ref} and V_{ref} are the related reference values, respectively. Note that in this simulation, the system states are again transferred to the origin.

As in Fig. 12, to verify the performance, we further test the solution using a sample 13-bus test system following [40]. The test system has 5 DGs and 6 loads. In the illustrated system, we assume that the proposed solution is applied to DG5 with 60Hz and 1p.u. being the related reference values, and the other DGs are only droop-controlled (i.e., primary control). Therefore, the system frequency will be regulated to its reference, and meanwhile the voltages are regulated by setting the voltage of one DG to be the reference value. The DG capacity is 100 kVA. The R/X ratio of transmission lines is 0.8354 [40]. The system is operated in the islanded mode at 0s. The objective of the proposed solution is to learn $u_{p,i}$ and $u_{q,i}$ in (22) for DG5 so as to regulate the frequency and its voltage to the reference values. The training set is generated by randomly perturbing the islanded microgrid model. In sequence, the learned control laws are used to control DG5.

The results are given in Figs. 13 - 15. Fig. 13 shows the vector field of DG5, where the red point is the origin (i.e., $\Delta\omega = \omega_5 - \omega_{\text{ref}} = 0$, $\Delta V = V_5 - V_{\text{ref}} = 0$). Assuming the system faces a large disturbance, we compare our solution with LQR control. The upper figures in Fig. 14 and Fig. 15 show the frequency and voltage magnitudes using LQR control. The lower figures in Fig. 14 and Fig. 15 illustrate the results with the learned control laws. As in the results, our solution can maintain the system states within the operational range and outperforms LQR control. Since LQR control is designed for linearized systems, its performance may deteriorate when facing large power changes or model uncertainties. Our solution is model-free, and its correctness has been proved over the entire state region. Therefore, it would have better performance in addressing various disturbances.

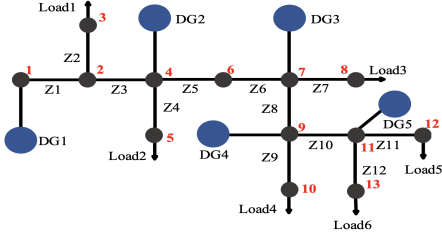


Fig. 12. The sample 13-bus test system [40]

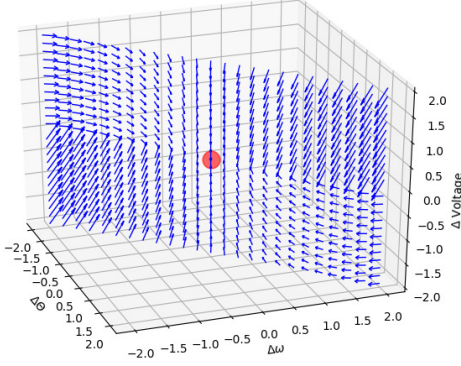


Fig. 13. The vector field of DG5 in Application II

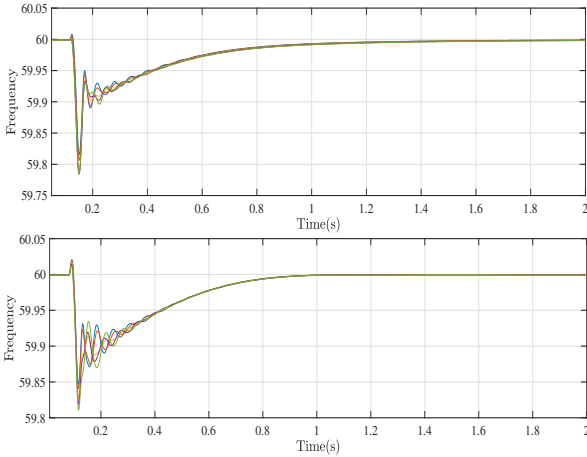


Fig. 14. Frequency profiles of DGs in Application II: a) LQR-based solution b) the proposed solution

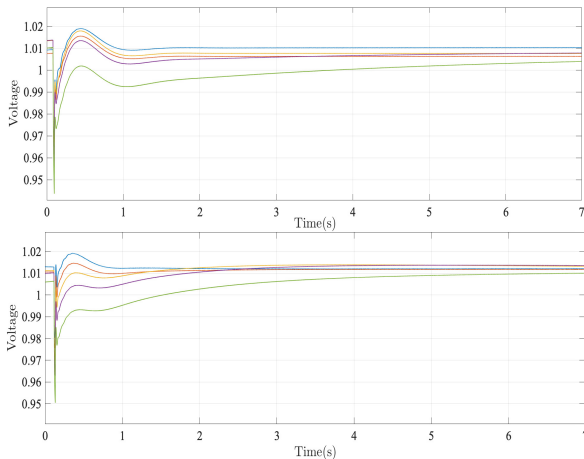
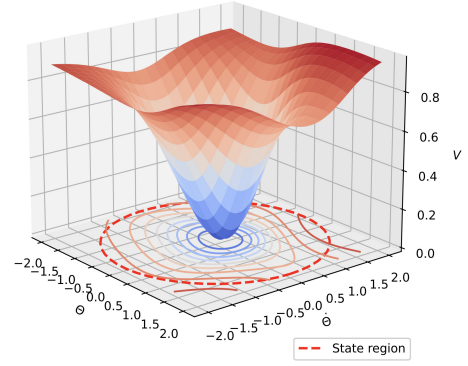
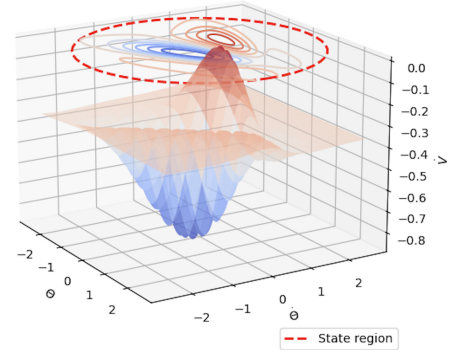


Fig. 15. Voltage profiles of DGs in Application II: a) LQR-based solution b) the proposed solution



(a) Learned Lyapunov function



(b) The derivative of the learned Lyapunov function

Fig. 16. The results in Application III: $V_\epsilon > 0$ in the upper figure and $\nabla_{f(x,\Psi)} V_\epsilon < 0$ in the lower figure

C. Application III: Power systems with heterogeneous inter-face dynamics

In this case study, we test our solution on the IEEE 123-node test feeder. It consists of 3 MGs and 2 traditional SGs modified from [12], leading to the heterogeneous dynamics. The MGs are connected to the grid via an inverter-interface with angle droop control [12], and the dynamics of SGs are governed by (20).

We consider MG 3 is isolated from the grid at $t = 0$ and control the rest of the MGs and SGs to maintain stability. Figs. 16(a)-16(b) illustrate the results of the learned Lyapunov function and its derivative for an SG. Fig.16(a) verifies the learned function is positive definite, i.e., $V_\epsilon(x) > 0$ and Fig. 16(b) shows its derivative is negative definite, i.e., $\nabla_{f(x,\Psi)} V_\epsilon(x) < 0$. Therefore, we can conclude our solution is able to find Lyapunov functions for a complicated system. Fig.17 shows the evaluation of system states when applying our control laws. As shown in the results, the system maintains synchronization when MG 3 disconnects from the grid. The above findings demonstrate our solution is capable of dealing with problems with the heterogeneous dynamics in a large test system.

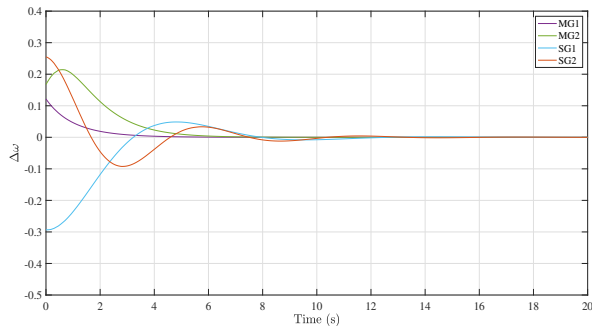


Fig. 17. State evaluation in Application III

D. Discussion

The above case studies demonstrate the effectiveness of our solution from 1) the ability to discover a valid Lyapunov function and control laws for various problems, 2) an enlarged ROA compared with the existing works, and 3) the capability of handling the heterogeneous interface dynamics. The proposed framework could simplify the analysis tools for nonlinear power system problems, providing the correctness guarantee and model-free feature.

The statistics of applying our solution to different example models are summarized in Table II. Note that the learning time in Table II only reflects the offline computational time. In a real-time implementation, the running time shows our solution is able to be implemented in real-time for a large system, which is also verified by the results in Application III. Intuitively, a large model leads to a long learning time since a large number of neurons are understandably needed in Learning Module. We would like to highlight that the trade-off between more layers needed to compute a Lyapunov function over a large searching domain and the learning speed should be optimized towards higher training efficiency.

Remark 4.2: The proposed framework is also applicable to the stability analysis of large-scale systems. We can adjust the size of the neural network and its hidden layer to capture more complicated states of large systems and use Falsification Module to ensure correctness following the procedure in Section III.D. It should be noted that increasing the size of neural networks would lead to a long learning time needed in Learning Module as discussed in Section IV.D. Improving computational efficiency and maintaining the effectiveness of large systems would be one of our future directions.

TABLE II
STATISTICS OF LEARNING DIFFERENT TEST MODELS

Test model	δ	Initial samples	Falsification samples	Learning time	Running time
1-machine system	0.01	300	234	12.5s	0.062s
3-bus system [41]	0.01	300	634	31.5s	0.086s
13-bus system	0.01	500	1083	315s	0.122s
39-bus system	0.01	1000	4668	1264s	0.393s
123-bus system	0.01	2000	9668	2764s	0.585s

V. CONCLUSION

This paper proposes a neural power system control framework leveraging a deep learning approach to closing the exist-

ing gaps in power system stability. It can deal with a variety of problems in power system control and stability analysis. The proposed framework can produce the valid Lyapunov function and control law simultaneously. The combination of learning and falsification modules guarantees the system stability and further demonstrates the performance of the obtained function over the verified domain. With the flexible structure of the framework, the control design for a typical power system problem is significantly simplified while providing a larger ROA. Several case studies are carried out to verify the effectiveness of the proposed framework in different problems.

VI. ACKNOWLEDGMENT

This material is based upon work supported by the U.S.Department of Energy’s Office of Energy Efficiency and Renewable Energy(EERE) under the Solar Energy Technologies Office Award Number 34230.

APPENDIX

A. Proof of Theorem 3.1

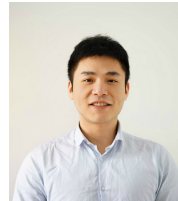
The proof includes three criteria according to [42].

- 1) The convexity of ICNN ensures the single optimum of V_ϵ and by (10), it further guarantees $V_\epsilon(0) = 0$.
- 2) The termination of the learning process, i.e., Falsification Module returns unsatisfaction, shows that $x \in \{x \in \mathcal{X} \setminus 0 \mid V_\epsilon(x) > 0 \text{ and then } \nabla_{f(x,\Psi)} V_\epsilon(x) < 0\}$, which is ensured by the correctness of the SMT solver [31]
- 3) Combining the above two criteria shows that the validated Lyapunov function V_ϵ with the corresponding control law Ψ holds the Lyapunov conditions. One can conclude the system is asymptotically stable with V_ϵ being a Lyapunov function [42].

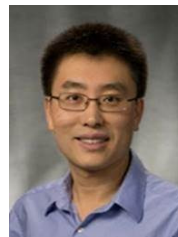
REFERENCES

- [1] P. Kundur, J. Paserba, V. Ajjarapu, G. Andersson, A. Bose, C. Canizares, N. Hatziargyriou, D. Hill, A. Stankovic, C. Taylor *et al.*, “Definition and classification of power system stability ieeecigre joint task force on stability terms and definitions,” *IEEE transactions on Power Systems*, vol. 19, no. 3, pp. 1387–1401, 2004.
- [2] C. Mishra, A. Pal, J. S. Thorp, and V. A. Centeno, “Transient stability assessment of prone-to-trip renewable generation rich power systems using lyapunov’s direct method,” *IEEE Transactions on Sustainable Energy*, vol. 10, no. 3, pp. 1523–1533, 2019.
- [3] Y. Zhang and L. Xie, “Online dynamic security assessment of microgrid interconnections in smart distribution systems,” *IEEE Transactions on Power Systems*, vol. 30, no. 6, pp. 3246–3254, 2014.
- [4] Z. Wang, F. Liu, S. H. Low, C. Zhao, and S. Mei, “Distributed frequency control with operational constraints, part i: Per-node power balance,” *IEEE Transactions on Smart Grid*, vol. 10, no. 1, pp. 40–52, 2017.
- [5] Y. Mi, Y. Fu, C. Wang, and P. Wang, “Decentralized sliding mode load frequency control for multi-area power systems,” *IEEE Transactions on Power Systems*, vol. 28, no. 4, pp. 4301–4309, 2013.
- [6] T. Stegink, C. De Persis, and A. van der Schaft, “A unifying energy-based approach to stability of power grids with market dynamics,” *IEEE Transactions on Automatic Control*, vol. 62, no. 6, pp. 2612–2622, 2016.
- [7] T. L. Vu and K. Turitsyn, “Lyapunov functions family approach to transient stability assessment,” *IEEE Transactions on Power Systems*, vol. 31, no. 2, pp. 1269–1277, 2015.
- [8] H. Liu, Z. Hu, and Y. Song, “Lyapunov-based decentralized excitation control for global asymptotic stability and voltage regulation of multi-machine power systems,” *IEEE Transactions on Power Systems*, vol. 27, no. 4, pp. 2262–2270, 2012.

- [9] E. Mallada, C. Zhao, and S. Low, "Optimal load-side control for frequency regulation in smart grids," *IEEE Transactions on Automatic Control*, vol. 62, no. 12, pp. 6294–6309, 2017.
- [10] A. J. Wood, B. F. Wollenberg, and G. B. Sheblé, *Power generation, operation, and control*. John Wiley & Sons, 2013.
- [11] Y. Guo, D. J. Hill, and Y. Wang, "Global transient stability and voltage regulation for power systems," *IEEE Transactions on Power Systems*, vol. 16, no. 4, pp. 678–688, 2001.
- [12] Y. Zhang and L. Xie, "A transient stability assessment framework in power electronic-interfaced distribution systems," *IEEE Transactions on Power Systems*, vol. 31, no. 6, pp. 5106–5114, 2016.
- [13] Y. Pan, L. Chen, X. Lu, J. Wang, F. Liu, and S. Mei, "Stability region of droop-controlled distributed generation in autonomous microgrids," *IEEE Transactions on Smart Grid*, vol. 10, no. 2, pp. 2288–2300, 2018.
- [14] J. W. Simpson-Porco, F. Dörfler, and F. Bullo, "Voltage stabilization in microgrids via quadratic droop control," *IEEE Transactions on Automatic Control*, vol. 62, no. 3, pp. 1239–1253, 2016.
- [15] L. Zhu, D. J. Hill, and C. Lu, "Hierarchical deep learning machine for power system online transient stability prediction," *IEEE Transactions on Power Systems*, vol. 35, no. 3, pp. 2399–2411, 2019.
- [16] G. Zhang, W. Hu, D. Cao, Q. Huang, J. Yi, Z. Chen, and F. Blaabjerg, "Deep reinforcement learning-based approach for proportional resonance power system stabilizer to prevent ultra-low-frequency oscillations," *IEEE Transactions on Smart Grid*, vol. 11, no. 6, pp. 5260–5272, 2020.
- [17] Y. Zhang, C. Chen, G. Liu, T. Hong, and F. Qiu, "Approximating trajectory constraints with machine learning microgrid islanding with frequency constraints," *IEEE Transactions on Power Systems*, 2020.
- [18] Z. Yan and Y. Xu, "Data-driven load frequency control for stochastic power systems: A deep reinforcement learning method with continuous action search," *IEEE Transactions on Power Systems*, vol. 34, no. 2, pp. 1653–1656, 2018.
- [19] Y. Zhang, X. Wang, J. Wang, and Y. Zhang, "Deep reinforcement learning based volt-var optimization in smart distribution systems," *arXiv preprint arXiv:2003.03681*, 2020.
- [20] A. J. Taylor, V. D. Dorobantu, H. M. Le, Y. Yue, and A. D. Ames, "Episodic learning with control lyapunov functions for uncertain robotic systems," *arXiv preprint arXiv:1903.01577*, 2019.
- [21] P. Yang, F. Liu, Z. Wang, and C. Shen, "Distributed stability conditions for power systems with heterogeneous nonlinear bus dynamics," *IEEE Transactions on Power Systems*, vol. 35, no. 3, pp. 2313–2324, 2020.
- [22] Y.-C. Chang, N. Roohi, and S. Gao, "Neural lyapunov control," pp. 3245–3254, 2019. [Online]. Available: <http://papers.nips.cc/paper/8587-neural-lyapunov-control.pdf>
- [23] S. Gao, J. Avigad, and E. M. Clarke, " δ -complete decision procedures for satisfiability over the reals," in *International Joint Conference on Automated Reasoning*. Springer, 2012, pp. 286–300.
- [24] Z. Arstein, "Stabilization with relaxed controls," *Nonlinear analysis*, vol. 7, no. 11, pp. 1163–1173, 1983.
- [25] A. Kasis, E. Devane, C. Spanias, and I. Lestas, "Primary frequency regulation with load-side participation—part i: Stability and optimality," *IEEE Transactions on Power Systems*, vol. 32, no. 5, pp. 3505–3518, 2017.
- [26] H. R. Baghaee, M. Mirsalim, and G. B. Gharehpetian, "Power calculation using rbf neural networks to improve power sharing of hierarchical control scheme in multi-der microgrids," *IEEE Journal of Emerging and Selected Topics in Power Electronics*, vol. 4, no. 4, pp. 1217–1225, 2016.
- [27] H. R. Baghaee, M. Mirsalim, G. B. Gharehpetian, and H. A. Talebi, "Nonlinear load sharing and voltage compensation of microgrids based on harmonic power-flow calculations using radial basis function neural networks," *IEEE Systems Journal*, vol. 12, no. 3, pp. 2749–2759, 2018.
- [28] B. Amos, L. Xu, and J. Z. Kolter, "Input convex neural networks," in *Proceedings of the 34th International Conference on Machine Learning—Volume 70*. JMLR. org, 2017, pp. 146–155.
- [29] J. Z. Kolter and G. Manek, "Learning stable deep dynamics models," in *Advances in Neural Information Processing Systems*, 2019, pp. 11 128–11 136.
- [30] C. Zhai and H. D. Nguyen, "Region of attraction for power systems using gaussian process and converse lyapunov function—part i: Theoretical framework and off-line study," *arXiv preprint arXiv:1906.03590*, 2019.
- [31] S. Gao, S. Kong, and E. M. Clarke, "dreal: An smt solver for nonlinear theories over the reals," in *International conference on automated deduction*. Springer, 2013, pp. 208–214.
- [32] H. R. Baghaee, M. Mirsalim, G. B. Gharehpetian, and H. A. Talebi, "A generalized descriptor-system robust h_∞ control of autonomous microgrids to improve small and large signal stability considering communication delays and load nonlinearities," *International Journal of Electrical Power & Energy Systems*, vol. 92, pp. 63–82, 2017.
- [33] M. Ayar, S. Obuz, R. D. Trevizan, A. S. Bretas, and H. A. Latchman, "A distributed control approach for enhancing smart grid transient stability and resilience," *IEEE Transactions on Smart Grid*, vol. 8, no. 6, pp. 3035–3044, 2017.
- [34] F. Dörfler and F. Bullo, "Synchronization and transient stability in power networks and nonuniform kuramoto oscillators," *SIAM Journal on Control and Optimization*, vol. 50, no. 3, pp. 1616–1642, 2012.
- [35] P. W. Sauer and M. A. Pai, *Power system dynamics and stability*. Wiley Online Library, 1998, vol. 101.
- [36] P. M. Anderson and A. A. Fouad, *Power system control and stability*. John Wiley & Sons, 2008.
- [37] F. Dörfler, M. R. Jovanović, M. Chertkov, and F. Bullo, "Sparsity-promoting optimal wide-area control of power networks," *IEEE Transactions on Power Systems*, vol. 29, no. 5, pp. 2281–2291, 2014.
- [38] H. Kwakernaak and R. Sivan, *Linear optimal control systems*. Wiley-interscience New York, 1972, vol. 1.
- [39] J. W. Simpson-Porco, Q. Shafiee, F. Dörfler, J. C. Vasquez, J. M. Guerrero, and F. Bullo, "Secondary frequency and voltage control of islanded microgrids via distributed averaging," *IEEE Transactions on Industrial Electronics*, vol. 62, no. 11, pp. 7025–7038, 2015.
- [40] Y. Du, X. Lu, J. Wang, and S. Lukic, "Distributed secondary control strategy for microgrid operation with dynamic boundaries," *IEEE Transactions on Smart Grid*, vol. 10, no. 5, pp. 5269–5282, 2019.
- [41] P. Yang, F. Liu, Z. Wang, and C. Shen, "Distributed stability conditions for power systems with heterogeneous nonlinear bus dynamics," *IEEE Transactions on Power Systems*, vol. 35, no. 3, pp. 2313–2324, 2019.
- [42] W. M. Haddad and V. Chellaboina, *Nonlinear dynamical systems and control: a Lyapunov-based approach*. Princeton university press, 2011.

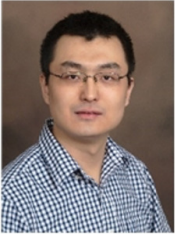


Tianqiao Zhao received his B.Eng. degree in automatic control from North China Electric Power University, Hebei, China, in 2013, and his PhD degree in electrical and electronic engineering from the University of Manchester, U.K., in 2019. From September 2018 to August 2019, he was a Postdoctoral Associate at Department of Electrical & Electronic Engineering, University of Manchester, UK. From September 2020 to February 2021, he was a Postdoctoral Fellow with the Department of Electrical and Computer Engineering at Southern Methodist University. He is currently with Brookhaven National Laboratory as Research Associate. His research interests include distributed optimization and control, microgrid, and energy storage systems.



Jianhui Wang Dr. Jianhui Wang is a Professor with the Department of Electrical and Computer Engineering at Southern Methodist University. Dr. Wang has authored and/or co-authored more than 300 journal and conference publications, which have been cited for more than 30,000 times by his peers with an H-index of 87. He has been invited to give tutorials and keynote speeches at major conferences including IEEE ISGT, IEEE SmartGridComm, IEEE SEGE, IEEE HPSC and IGEC-XI.

Dr. Wang is the past Editor-in-Chief of the IEEE Transactions on Smart Grid and an IEEE PES Distinguished Lecturer. He is also a guest editor of a Proceedings of the IEEE special issue on power grid resilience. He is the recipient of the IEEE PES Power System Operation Committee Prize Paper Award in 2015, the 2018 Premium Award for Best Paper in IET Cyber-Physical Systems: Theory & Applications, the Best Paper Award in IEEE Transactions on Power Systems in 2020, and the IEEE PES Power System Operation, Planning, and Economics Committee Prize Paper Award in 2021. Dr. Wang is a Clarivate Analytics highly cited researcher for production of multiple highly cited papers that rank in the top 1% by citations for field and year in Web of Science (2018-2020). He is a Fellow of IEEE.



Xiaonan Lu (S'12-M'13) received his B.E. and Ph.D. degrees in electrical engineering from Tsinghua University, Beijing, China, in 2008 and 2013, respectively. From September 2010 to August 2011, he was a guest Ph.D. student at the Department of Energy Technology, Aalborg University, Denmark. From October 2013 to December 2014, he was a Postdoc Research Associate at the Department of Electrical Engineering and Computer Science, University of Tennessee, Knoxville. From January 2015 to July 2018, he was with Argonne National

Laboratory, first as a Postdoc Appointee and then as an Energy Systems Scientist. In July 2018, he joined the College of Engineering at Temple University as an Assistant Professor. His research interests include modeling and control of power electronic inverters, hybrid AC and DC microgrids, and real-time hardware-in-the-loop simulation. Dr. Lu is the Associate Editor of IEEE Transactions on Industrial Electronics, the Associate Editor of IEEE Transactions on Industry Applications, and the Editor of IEEE Transactions on Smart Grid. He serves as the Vice Chair of the Industrial Power Converters

Committee (IPCC) in the IEEE Industry Applications Society (IAS). He is also the recipient of the 2020 Young Engineer of the Year Award in the IEEE Philadelphia Section.



Yuhua Du (S'17-M'21) received the B.S degree in electrical engineering from Xi'an Jiaotong University, China in 2013 and Ph.D. degree in electrical and computer engineering from North Carolina State University, USA in 2019. He was a Research Aide with Argonne National Laboratory in 2018. He is currently a Postdoctoral Fellow at Temple University. His research interests include voltage source converter modeling and control, microgrid distributed secondary control and development of

microgrid hardware-in-the-loop testbed.